A Microwave Frequency Range Experiment for the Measurement of Snow Density and Liquid Water Content

Cédric Bermond ⓘ, Philippe Artillan ⓘ, and Michel Gay, *Member, IEEE*

Abstract—**This article presents a new nondestructive characterization system for the extraction of both snow density and liquid water content (LWC). The experiment primarily measures the relative complex permittivity of snow ($\overline{\varepsilon_s}$) at microwave frequencies at 4–6 GHz. The density and LWC are then deduced with high accuracy from an empirical model of the literature that has been experimentally validated in this study.**

Index Terms—**Complex permittivity, density, high-frequency characterization, liquid water content (LWC), snow, snowpack.**

I. INTRODUCTION

THE KNOWLEDGE of the snow water equivalent (SWE) of a snowpack, or in an equivalent manner, its effective density ρ_s, is important to predict the water resources in the mountains, especially for hydroelectric dams [1], [2]. The effective density typically varies from 0.1 to 0.6 g/cm^3. Furthermore, a complete description of the state of the snow must include its liquid water content (LWC), or wetness. The LWC, or wetness, allows for the classification of snow in three categories according to the volumetric water. Dry snow is described with LWC = 0, wet snow with LWC = 1–8%, and very wet snow with LWC = 8–15%. These data can be obtained by traditional snow pit observations or by several kinds of electromagnetic measurement methods, which are all based on the relation between the complex permittivity ($\overline{\varepsilon_s} = \varepsilon'_s - j\varepsilon''_s$) and the duplet ($\rho_s$, LWC).

First, measurements of the complex permittivity can be directly performed by an operator using a capacitive sensor [3], or a resonant cavity [4]. In order to allow easy, automatic, and nondestructive measurements, free-space methods, involving ground-directed antennas have been developed. The first method is based on a ground-penetrating radar (GPR), which measures the propagation velocity of an electromagnetic pulse in the

snowpack [5]–[7]. A second approach is to use a wideband frequency-modulated continuous-wave (FM-CW) radar [8], [9]. The analysis of the delay of reflected signals allows us to describe the physical layers in terms of changes in real dielectric permittivity. These radars propose a remote monitoring system for the depth of snow [10] or even the snowpack stratigraphy [11]. Finally, the possibility to use an electromagnetic test bench using a vector network analyzer (VNA) to extract very precisely, the effective density from the real part of the dielectric permittivity has been demonstrated for a dry snowpack in [12] and [13]. However, all these methods only measure a delay time or a phase shift, thus only allowing the determination of the real part of the snow permittivity ε'_s. In previous references, the density ρ_s was deduced from this measurement by assuming dry snow (LWC = 0%). Other methods extract LWC, assuming a known average density for snow ρ_s [14].

In this article, we propose a nondestructive test bench operating in the 4–6 GHz range, based on a two-port VNA two-horn antennas setup, measuring the full scattering matrix of a snow sample. A VNA uses a continuous wave frequency sweep without frequency modulation. The sensitivity of VNA measurements is much higher than GPR (the dynamic range reaches 80 dB) and the extraction gives information on both the magnitude and the phase of the signal. Both the real and the imaginary parts of the permittivity can then be extracted, thus allowing for the determination of both the snow density ρ_s and its LWC.

This article is divided into four parts. Section II presents the frequency-dependent model of permittivity used to extract the density and the LWC. Section III describes the test bench and details the calibration procedure with the extraction algorithm. A theoretical demonstration estimates the measurement error and the impact on the extraction of the permittivity. Section IV discusses the density and LWC results, for wet and dry snow. Finally, we will compare the density extract from measurement with the complex permittivity to the density extract from manual measurement.

II. SNOW PERMITTIVITY MODEL

Several models have been established that describe the complex permittivity of snow $\overline{\varepsilon_s} = \varepsilon'_s - j\varepsilon''_s$ [15]–[17]. Dry snow can be described by Matzler's model [18], which only depends on the density. The model proposed by Sihvola and Tiuri [19]

Fig. 1.   Imaginary part of the snow permittivity for different values of LWC.

Fig. 2.   Real part of the snow permittivity for two values of density and three values of LWC.

also takes into account the LWC of the snow and has, thus, been chosen for our study. For the sake of completeness, the empirical equations that relate to snow density ρ_s and LWC W (in % of the total volume) to the complex permittivity are rewritten as

$$\varepsilon_s' = \left(0.1W + 0.8W^2\right) \varepsilon_w'$$
$$+ \left(1 + 1.7\left(\rho_s - W\right) + 0.7(\rho_s - W)^2\right) \quad (1)$$

$$\varepsilon_s'' = \left(0.1W + 0.8W^2\right) \varepsilon_w''. \quad (2)$$

It is convenient to express the relative permittivity of the water in terms of a complex number with $\overline{\varepsilon_w} = \varepsilon_w' - j\varepsilon_w''$. The Debye relaxation allows us to compute $\overline{\varepsilon_w}$

$$\overline{\varepsilon_w} = \varepsilon_{w\infty} + \frac{\varepsilon_{w\mathrm{dc}} - \varepsilon_{w\infty}}{1 + j\omega\tau} \quad (3)$$

with ω as the angular frequency $\omega = 2\pi f$ and f is the frequency, τ is the relaxation time, $\varepsilon_{w\infty}$ is the optical (infinite frequency) dielectric constant for $f = \infty$, and $\varepsilon_{w\mathrm{dc}}$ is the static value of the dielectric constant for $f = 0$. The temperature effect on relaxation time and for 0 °C, we use $\tau = 17$ ps, $\varepsilon_{w\infty} = 4.9$, and $\varepsilon_{w\mathrm{dc}} = 88$.

On one hand, the imaginary part of the snow permittivity only depends on the LWC. The imaginary part of permittivity of the snow becomes high enough for extraction above 1 GHz and it remains almost linear with frequency up to 6 GHz as shown in Fig. 1. Moreover, the electromagnetic wave penetration depth between 1 and 6 GHz allows samples to be a few centimeters thick. We thus decided to use this frequency range to extract LWC with good accuracy.

On the other hand, the real part of the snow permittivity depends on both its density and its LWC, as shown in Fig. 2. Below 1 GHz, the real part stays constant with frequency. Above 1 GHz, its behavior strongly depends on the LWC: The higher the LWC, the lower the real part of the permittivity. In order to obtain the density of the snow with good accuracy, the LWC must then be extracted before dielectric losses. Very low LWC values such as 0.1% correspond to extracting a very low imaginary part of the permittivity at the chosen frequency range such as 2×10^{-3}, which is hardly attainable with a field experiment.
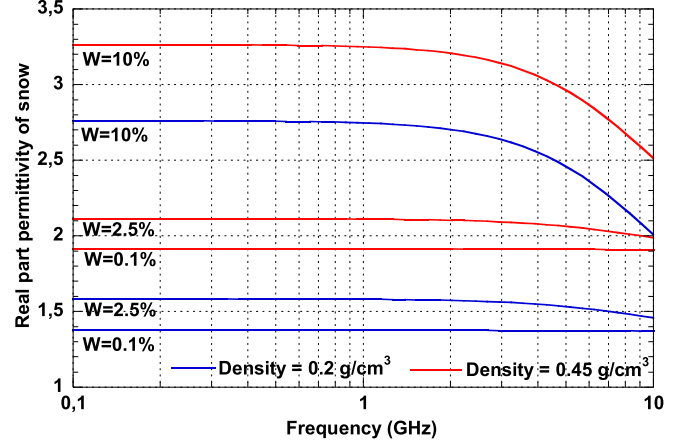
However, the high sensitivity of the proposed test bench, which is due to the combination of using a free-space method (no air gaps between the sample and the measurement device) and an accurate VNA, allows extracting LWC values greater than or equal to 1% (corresponding to determining imaginary part of permittivity upper than 2×10^{-2}).

We can compute the LWC and the density by inverting the empirical equations given in (1) and (2)

$$W = \frac{\sqrt{\varepsilon_w''^2 + 320\,\varepsilon_w''\,\varepsilon_s''} - \varepsilon_w''}{16\,\varepsilon_w''} \quad (4)$$

$$\rho_s = W + \frac{1}{14}\sqrt{-224\,\varepsilon_w'\,W^2 - 28\,\varepsilon_w'W + 280\,\varepsilon_s' + 9} - \frac{17}{4}. \quad (5)$$

The next part expounds on our free-space test bench with the complex permittivity extraction procedure.

III. MEASUREMENT SETUP

A. Test Bench Description

As presented in fig. 3, a portable complex permittivity measurement bench has been realized. Two rectangular horn antennas (Pasternack PE9861) are connected to a VNA. The measurements of the two-port scattering parameters have been performed in the 4–6 GHz frequency range. The material under test (MUT) is a parallelepipedic sample of about 50 cm × 50 cm and of variable thickness l placed between the two antennas. The antennas must be highly directional (20 dB) to focus the electromagnetic field into the sample and to avoid secondary reflections on the sides of the experiment. Furthermore, the parasitic standing wave due to secondary reflections must be minimized by protecting the metallic supports with absorbers. Finally, one antenna is placed on a micropositioning system in order to provide fine tuning of the distance between the two antennas for TRL calibration.

Fig. 3.   Portable complex permittivity measurement bench.

B. Plane-Wave Approximation

The procedure of material permittivity extraction is based on the plane-wave approximation. The electromagnetic wave generated by the horn antenna of our test bench has been simulated with Ansys Electronics Desktop HFSS solver in order to determine the minimum distance to place the sample, still verifying the plane-wave hypothesis. Fig. 4(a) presents the magnitude of the electrical field. Its distribution on a transverse section is almost Gaussian with a maximum at the center *z*-axis. Although this is not strictly a plane-wave configuration, the fact that almost all the energy is concentrated on the central axis and is then retrieved in the receiving horn antenna that makes the experiment correctly set up. The most important criteria to avoid interferences between the various paths for the wave is to keep the phase of the E-field almost constant on a transverse section. Fig. 4(b) shows that the difference of the E-field phase is inferior at $10°$ on the surface of the spot.

C. Test Bench Calibration and Complex Permittivity Extraction Procedure

The TRL calibration technique [20], [21] is well appropriate for free-space measurements because the calibration standards (Thru, Reflect, Line) are easily realized and the characteristic impedance of the propagating waves in free space is well known. This procedure is developed without time gating and is performed in three steps (cf. Fig. 5).

The Reflect standard [see Fig. 5(a)] consists of a metal plate of thickness $l_{\text{REFLECT}} = 5$ mm, placed between the two antennas. It allows setting the position of the reference planes for the measurement.

The Line standard [see Fig. 5(b)] is obtained by removing the reflect standard, the distance between the horn antennas being unchanged. The length of the line standard must verify the following relationship for any angular frequency ω to avoid phase mistakes in calibration errors terms:

$$20° < \frac{\omega}{c_0} l_{\text{REFLECT}} < 160° \tag{6}$$

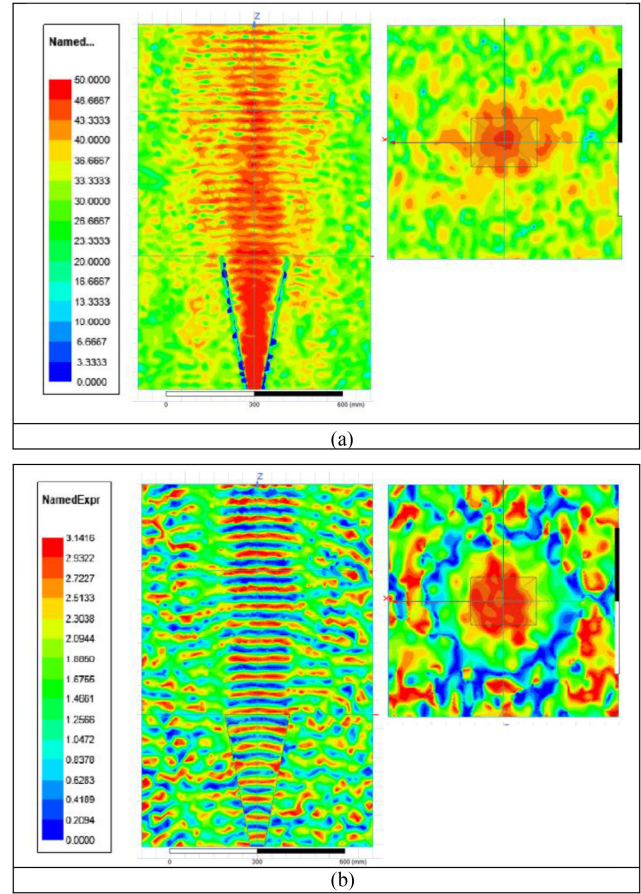where $c_0 = 3 \times 10^8$ ms^{-1}.

Fig. 4.   Numerical modelization of the *y*-component of the electrical field generated by the horn antenna. (a) Magnitude in decibel. (b) Phase (absolute value, in radians).

The Thru standard [see Fig. 5(c)] is achieved by moving one antenna forward of the thickness of the Reflect standard.

We then used the Ross–Nicholson–Weir method [22]–[24] to extract the relative complex permittivity of the MUT. The reference planes are first placed at each side of the MUT sample by measurement postprocessing. The reflection and transmission coefficients of the MUT sample are then computed from the four scattering parameters. The complex permittivity is then extracted from the transmission coefficient. The reflection coefficient could be used for high real permittivity samples, but for snowlike materials, the best results are obtained from the transmission coefficient.

D. Extraction Uncertainty Computation

The uncertainties of the extraction mainly come from the uncertainty of the sample's thickness Δl and the uncertainty of the phase $\Delta \theta$ of the transmission scattering parameter $S_{21} = |S_{21}| \ e^{j\theta}$. Here, we propose a simple computation, based on realistic approximations, of the impact of measurement uncertainties Δl and $\Delta \theta$ on the real part of the snow permittivity ε_s'.

For simplicity's sake, instead of using the complex permittivity $\overline{\varepsilon_s}$, the computation is made with the complex refractive
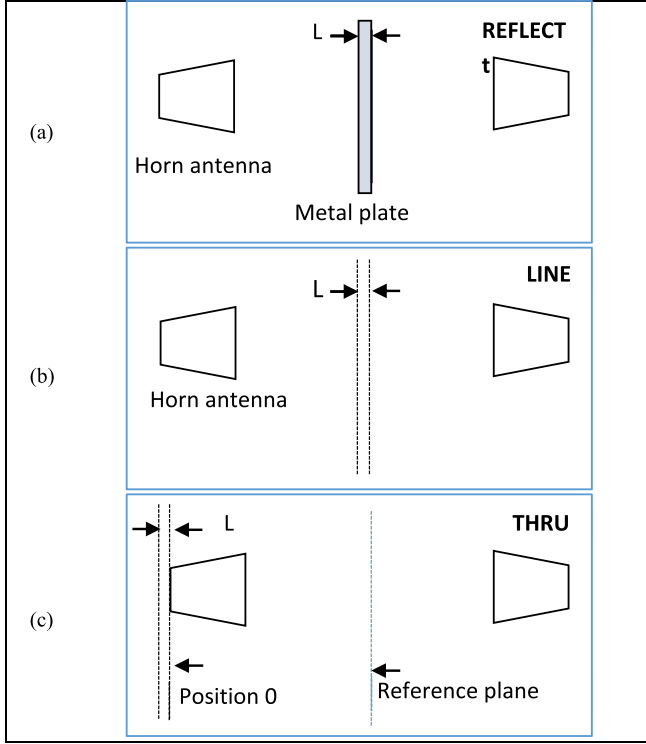
Fig. 5. TRL calibration standards. (a) Reflect. (b) Line. (c) Thru.

index $\bar{n}$

$$\bar{n} = \sqrt{\bar{\varepsilon_s}} = n - jk. \tag{7}$$

The coefficient of transmission t is defined as

$$t = e^{-j\frac{\omega \bar{n} l}{c}} = e^{-\frac{\omega k l}{c}} \, e^{-j\frac{\omega n l}{c}}. \tag{8}$$

Assuming that the reflection coefficient is very small $0 < |r| \ll 1$, the transmission coefficient t can be assimilated to the transmission scattering parameter S_{21}

$$t \approx \frac{(1 - r^2) t}{1 - r^2 t^2} = S_{21} = |S_{21}| \, e^{j\theta}. \tag{9}$$

The relation between n, θ, and l thus becomes

$$\theta \approx \frac{\omega n l}{c} \tag{10}$$

and the uncertainty on the real part of the refractive index can be written as

$$\Delta n \approx \frac{c}{\omega l} \Delta \theta + n \frac{\Delta l}{l}. \tag{11}$$

To estimate the typical error of extraction, we used the value of real permittivity of dry snow $n = \sqrt{1.6}$ and a thickness of sample with 210 mm. The value $\Delta\theta$ represents the variation of phase during measurement due to the temperature stability of the VNA. We maximize this value with $\Delta\theta = 0.5°$. We consider an error of length during the measurement of the sample $\Delta l = 5$ mm. For a frequency of 5 GHz, the error on the permittivity is less than 3%. This result demonstrates the accuracy of the proposed method.
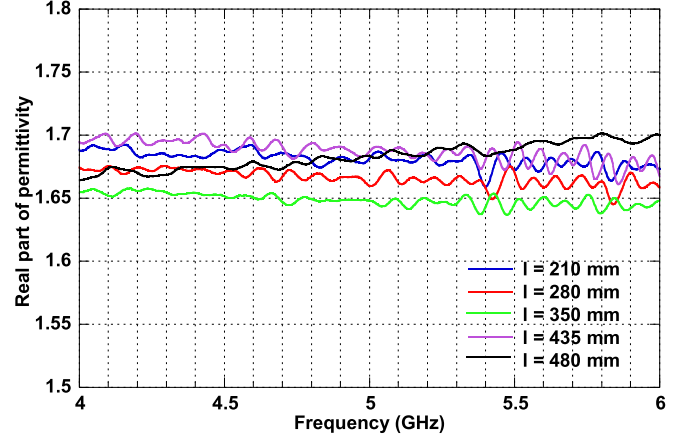

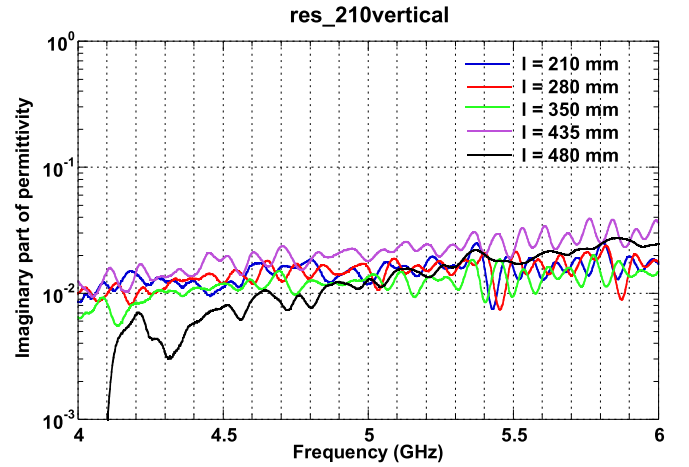Fig. 6. Real-part permittivity of snow from five samples for a density of 0.34 g/cm^3.

Fig. 7. Imaginary-part permittivity of snow from five samples for a density of 0.34 g/cm^3.

IV. RESULTS

A. Preliminary Results on Dry Snow and System Performances

In order to validate the accuracy of the test bench, measurements have been performed with five different samples' thicknesses. These measurements were acquired in the massif of Mont Blanc on the roof of the Argentière hut at an altitude of 2700 m (11/11/2020). The snow is considered dry (LWC = 0). The density of the snow was measured at 0.34 g/cm^3 and the temperature of the snow was measured at -3 °C. We can notice a high precision of measurement with less than 3% of variation on the real part of permittivity as shown in Fig. 6.

Although the snow is considered dry, the imaginary part of the complex permittivity is not exactly zero as shown in Fig. 7. The free-space transmission system then has a noise floor and cannot measure values of imaginary parts of permittivity lower than 10^{-2}.

From the relationship (4) and (5), the LWC and the density were extracted on the frequency range. Fig. 8 shows these results for five samples from 210 to 480 mm thick.
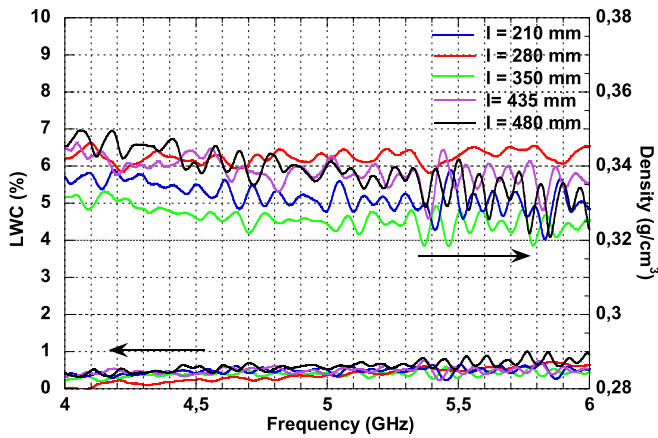
Fig. 8.   LWC and density extracted from measurement for dry snow.

TABLE I
LWC AND DENSITY EXTRACTED FROM MEASUREMENTS

Thickness	Measurements (4 GHz - 6 GHz)		Error relative of density (direct measurement 0.34 g/cm³)
	Average LWC (%)	Average density (g/cm³)	
210 mm	0.45	0.339	0.6%
280 mm	0.42	0.333	2%
350 mm	0.35	0.327	3.8%
435 mm	0.60	0.332	2.3%
480 mm	0.36	0.342	0.6%

The density is quite constant versus frequency. The ripple can be explained by the impact of parasitic waves during the measurement. This phenomenon is low and represents only 5% of the average value. The LWC stays constant with the frequency with an average value of 0.5%. Both results demonstrate the accuracy of our test bench.

Table I gives the average value of LWC extracted from the imaginary part of the complex permittivity for the five samples.
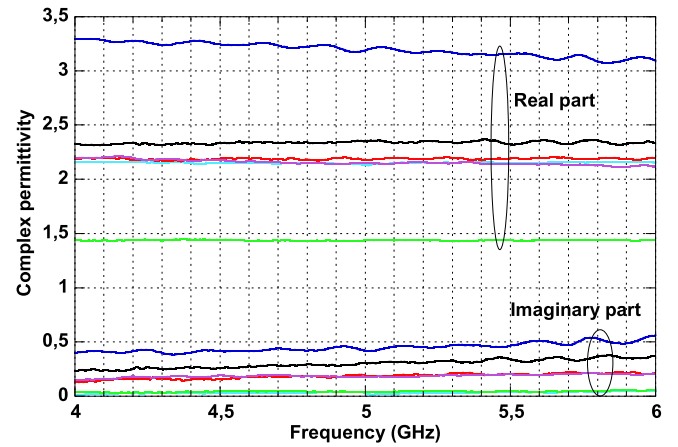
First, the values are little but not zero for LWC. The empirical noise floor of the test bench is then evaluated to 0.6% for the LWC. Second, the measurement system is qualified to measure the density of snow with less than 5% error.

B. Characterization of Snow

In this part, we present the extraction of the density and the LWC of any kind of snow. Six samples have been measured, during winter and spring. The complex permittivity of each sample was extracted between 4 and 6 GHz. The extraction process is illustrated as shown in Fig. 9. The real part varies between 1.4 and 3.3, corresponding to an increasing density. The imaginary part varies between 0.01 and 0.6 and suggests moisture in the samples.

From these results, the LWC and the density were then extracted with the relationships (4) and (5) and are presented in Figs. 10 and 11.

As the frequency behavior of the LWC is flat, we have extracted an average value of 4.66% for one sample (Col de Porte 02/26/2021). A commercial sensor named WISE [25], based on

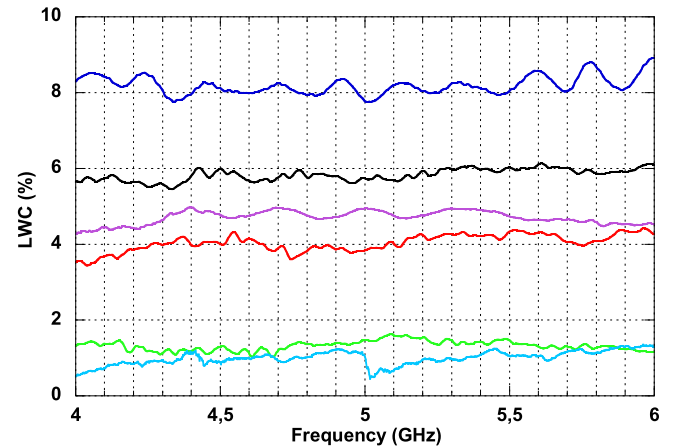|	Date	Place		Date	Place
■ (blue)	05/18/20	Val Thorens	■ (green)	01/15/2021	Pipay
■ (red)	02/08/21	Pipay	■ (magenta)	02/26/2021	Col de Porte
■ (black)	02/08/21	Pipay	■ (cyan)	04/23/2021	Argentière

Fig. 9.   Complex permittivity of snow samples.

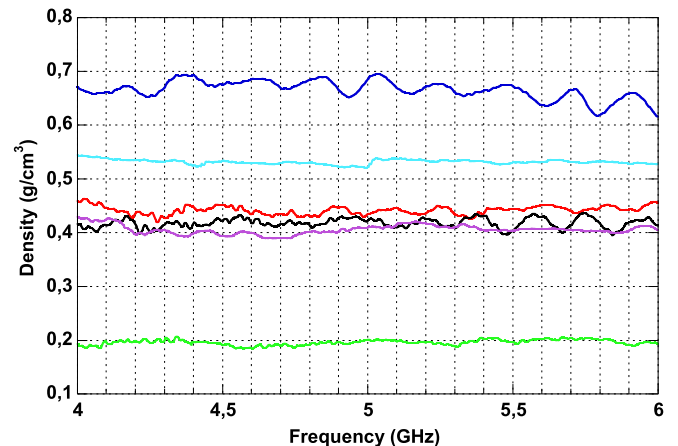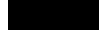Fig. 10.   LWC extracted from the measurement of the samples of snow.

Fig. 11.   Density extracted from the measurement of the samples of snow.

TABLE II
SNOW MEASUREMENTS

Sample	Density (g/cm^3)		Error relative of density
	Direct measurement	Average density	
	0.625	0.665	6.4%
	0.417	0.441	5.7%
	0.391	0.408	4.2%
	0.200	0.196	2%
	0.410	0.405	1.2%
	0.521	0.531	1.9%

low-frequency capacitive measurement [26], has given a very close value of 4.88%, thus validating our approach. The error on LWC is less than 5%.

Each sample has been weighted and its volume has been measured to calculate its density. These values are compared to the extracted density from the high-frequency measurement of the complex permittivity in Table II. The density shows a very good agreement between measurement results with the high-frequency extraction and the theoretical model, thus validating the electromagnetic measurement setup and the reverse modeling extracting approach. The error on the density is less than 7%.

V. CONCLUSION

We have developed and validated a free-space test bench to measure the complex permittivity of snow with high accuracy between 4 and 6 GHz. This procedure is based on the measurement of scattering parameters of a snow sample and the use of a validated extraction algorithm. Snow properties are then deduced from complex permittivity measurements thanks to a reversed analytical model. On one hand, the density of dry or wet snow can be extracted with a precision of 7%. On the other hand, the LWC is precisely measured down to 1% by volume. This work enables the further objective to perform a permanent monitoring *in-situ* measurement of the effective complex permittivity of the snowpack, thus enabling the computation of the SWE.

REFERENCES

[1] D. Viviroli *et al.*, "Climate change and mountain water resources: Overview and recommendations for research, management and policy," *Hydrol. Earth Syst. Sci.*, vol. 15, no. 2, pp. 471–504, 2011.

[2] L. Egli *et al.*, "Comparison of different automatic methods for estimating snow water equivalent," *Cold Regions Sci. Technol.*, vol. 57, no. 2, pp. 107–115, 2009.

[3] M. Y. Louge *et al.*, "A portable capacitance snow sounding instrument," *Cold Regions Sci. Technol.*, vol. 28, pp. 73–81, 1998.

[4] A. E.-C. Tan *et al.*, "Microwave measurements of snow over sea-ice in Antarctica," in *Proc. 12th Int. Conf. Electromagn. Wave Interaction Water Moist Substances*, 2018, pp. 1–9.

[5] J. H. Bradford, J. L. Harper, and J. Brown, "Complex dielectric permittivity measurements from ground-penetrating radar data to estimate snow liquid water content in the pendular regime," *Water Resour. Res.*, vol. 45, 2009, Art. no. W08403.

[6] H. Liu, K. Takahashi, and M. Sato, "Measurement of dielectric permittivity and thickness of snow and ice on a Brackish Lagoon using GPR," *IEEE J. Sel. Topics Appl. Earth Observ. Remote Sens.*, vol. 7, no. 3, pp. 820–827, Mar. 2014.

[7] W. S. Holbrook *et al.*, "Estimating snow equivalent over long mountain transects using snowmobile-mounted ground-penetrating radar," *Geophysics*, vol. 81, no. 1, pp. 183–193, 2016.

[8] R. Okorn *et al.*, "Upward-looking L-band FMCW radar for snow cover monitoring," *Cold Regions Sci. Technol.*, vol. 103, pp. 31–40, 2014.

[9] H. P. Marshall *et al.*, "Snow stratigraphy measurements with high-frequency FMCW radar: Comparison with snow micro-penetrometer," *Cold Regions Sci. Technol.*, no. 47, pp. 108–117, 2007.

[10] P. Kanagaratnam, T. Markus, V. Lytle, B. Heavey, P. Jansen, and G. Prescott, "Ultrawideband radar measurements of thickness of snow over sea ice," *IEEE Trans. Geosci. Remote Sens.*, vol. 45, no. 9, pp. 2715–2724, Sep. 2007.

[11] A. Heilig, M. Schneebeli, and O. Eisen, "Upward-looking ground-penetrating radar for monitoring snowpack stratigraphy," *Cold Regions Sci. Technol.*, vol. 59, pp. 152–162, 2009.

[12] M. Parsian, M. Barbolini, F. Dell'Acqua, P. F. Espín-López, and L. Silvestri, "Snowpack monitoring using a dual-receiver radar architecture," *IEEE Trans. Geosci. Remote Sens.*, vol. 57, no. 2, pp. 1195–1204, Feb. 2019.

[13] P. F. Espin-Lopez and M. Pasian, "Determination of snow water equivalent for dry snowpacks using the multipath propagation of ground-based radars*," IEEE Geosci. Remote Sens. Lett.*, vol. 18, no. 2, pp. 276–280, Feb. 2021.

[14] C. Mitterer *et al.*, "Upward-looking ground-penetrating radar for measuring wet-snow proprieties," *Cold Regions Sci. Technol.*, vol. 69, pp. 129–138, 2011.

[15] M. E. Tiuri, A. Sihvola, E. Nyfors, and M. Hallikaiken, "The complex dielectric constant of snow at microwave frequencies," *IEEE J. Ocean. Eng.*, vol. JOE-9, no. 5, pp. 377–382, Dec. 1984.

[16] M. T. Hallikainen, F. Ulaby, and M. Abdelrazik, "Dielectric proprieties of snow in the 3 to 37 GHz range," *IEEE Trans. Antennas Propag.*, vol. AP-34, no. 11, pp. 1329–1340, Nov. 1986.

[17] W. Huining *et al.*, "Effective permittivity of dry in the 18 to 90 GHz range," *Prog. Electromagn. Res.*, vol. PIER 24, pp. 119–138, 1999.

[18] C. Mätzler, "Relation between grin-size and correlation length of snow," *J. Glaciol.*, vol. 48, no. 162, pp. 461–477, 2002.

[19] A. H. Sihvola and E. Tiuri, "Snow fork for field determination of the density and wetness profiles of a snowpack," *IEEE Trans. Geosci. Remote Sens.*, vol. GE-24, no. 5, pp. 717–721, Sep. 1986.

[20] G. F. Engen and C. A. Hoer, "Thru-reflect-line: An improved technique for calibrating the dual six port automatic network analyzer," *IEEE Trans. Microw. Theory Techn.*, vol. MTT-27, no. 12, pp. 987–993, Dec. 1979.

[21] H. Heuermann and B. Schiek, "Robust algorithms for Txx network analyzer self-calibration procedures," *IEEE Trans. Instrum. Meas.*, vol. 43, no. 1, pp. 18–23, Feb. 1994.

[22] A. M. Nicolson and G. F. Ross, "Measurement of the intrinsic properties of materials by time domain technique," *IEEE Trans. Instrum. Meas.*, vol. TIM-19, no. 4, pp. 377–382, Nov. 1970.

[23] W. B. Weir, "Automatic measurement of complex dielectric constant and permeability at microwave frequencies," *Proc. IEEE*, vol. 62, no. 1, pp. 33–36, Jan. 1974.

[24] J. Baker-Jarvis, M. D. Janezic, J. H. Grosvenor, and R. G. Geyer, "Transmission/reflection and short-circuit line methods for measuring permittivity and permeability," Tech. Note 1355, Nat. Inst. Standards Technol., Gaithersburg, MD, USA, Dec. 1993.

[25] [Online]. Available: https://a2photonicsensors.com/wise/

[26] A. Mavrovic, J.-B. Madore, A. Langlois, A. Royer, and A. Roy, "Snow liquid water content measurement using an open-ended coaxial probe (OECP)," *Cold Regions Sci. Technol.*, vol. 171, Mar. 2020, Art. no. 102958, doi: 10.1016/j.coldregions.2019.102958.

Cédric Bermond received the Ph.D. degree in electronic, optronic, and systems from the University of Savoie Mont Blanc, Chambéry, France, in 2001.

He is currently an Assistant Professor with the Characterization and Microwave Laboratory (IMEP-LAHC), University of Savoie Mont Blanc. His research interests include characterization materials with microwave measurement and electromagnetic modeling.

Philippe Artillan received the Ph.D. degree in microelectronics from Université de Toulouse, Toulouse, France, in 2008.

He was with the Institut de Microelectronique Electromagnétisme et Photonique – Laboratoire d'Hyperfréquences et de Caractérisation, Chambéry, France, as an Associate Professor in the Radio Frequency and Millimeter Department. His research interest includes passive components with a particular interest in electromagnetic modeling, broadband characterization, and material parameters extraction.

Michel Gay (Member, IEEE) received the Engineering degree in microelectronics from the Institute of Engineering Sciences of Montpellier, France, in 1987, and the Ph.D. degree in physics from the University Joseph Fourier, Grenoble, France, in 1999.

From 1979 to 1985, he was a Technician with the Institute of Botany and Teacher with the Academy of Montpellier. From 1988 to 2003, he was with Cemagref Grenoble, where he was an Electronics Engineer with the research unit of Torrential Erosion Snow and Avalanche. Since 2004, he has been employed as a Research Engineer with the CNRS Laboratory "Grenoble Image Parole Signal Automatique," Saint Martin D'Heres, France. He was the Co-Leader of four National Scientific projects and three European projects. His research interest includes image-processing synthetic aperture radar (SAR), applied to the monitoring of snow and glaciers.